Developmental Cell
Article

ClpP Mediates Activation of a Mitochondrial Unfolded Protein Response in *C. elegans*

Cole M. Haynes,[1] Kseniya Petrova,[1,2] Cristina Benedetti,[1,2] Yun Yang,[1] and David Ron[1,*]
[1]Kimmel Center for Biology and Medicine of the Skirball Institute and the Departments of Cell Biology and Medicine, New York University School of Medicine, New York, NY 10016, USA
[2]These authors contributed equally to this work.
*Correspondence: ron@saturn.med.nyu.edu
DOI 10.1016/j.devcel.2007.07.016

SUMMARY

The cellular response to unfolded and misfolded proteins in the mitochondrial matrix is poorly understood. Here, we report on a genome-wide RNAi-based screen for genes that signal the mitochondrial unfolded protein response (UPR^{mt}) in *C. elegans*. Unfolded protein stress in the mitochondria correlates with complex formation between a homeodomain-containing transcription factor DVE-1 and the small ubiquitin-like protein UBL-5, both of which are encoded by genes required for signaling the UPR^{mt}. Activation of the UPR^{mt} correlates temporally and spatially with nuclear redistribution of DVE-1 and with its enhanced binding to the promoters of mitochondrial chaperone genes. These events and the downstream UPR^{mt} are attenuated in animals with reduced activity of *clpp-1*, which encodes a mitochondrial matrix protease homologous to bacterial ClpP. As ClpP is known to function in the bacterial heat-shock response, our findings suggest that eukaryotes utilize component(s) from the protomitochondrial symbiont to signal the UPR^{mt}.

INTRODUCTION

The essential processes of protein folding, complex assembly, and degradation are compartmentalized in eukaryotic cells. Chaperones and proteases are selectively targeted to the cytosol, endoplasmic reticulum, and mitochondria, where they service unfolded and misfolded proteins in each compartment (Hartl and Hayer-Hartl, 2002; Bukau et al., 2006). Signal transduction pathways selectively couple perturbation in the protein-folding environment in a given organelle to the activation of genes that enhance the capacity for protein handling by that organelle. These pathways have come to be known as unfolded protein responses (UPRs), and their importance to cellular and organismal homeostasis has been well documented (reviewed in Barral et al., 2004; Ron and Walter, 2007).

First to be identified was a cytosolic pathway, known as the heat-shock response (Lindquist, 1986), followed by the discovery of a similar pathway in the endoplasmic reticulum (ER), the UPR^{er} (Gething and Sambrook, 1992). In both compartments, signaling is initiated by a shift in equilibrium between unfolded proteins and their chaperones and is terminated by restoration of that equilibrium. Components that function in the cytoplasmic and ER UPRs have been identified, but the regulatory links between the folding environment in the mitochondrial matrix and the nuclear genes that encode mitochondrial chaperones have remained poorly understood.

The mitochondrial proteome is constituted from a small number of highly expressed mitochondrial genes and a large number of nuclear genes whose products are imported into the organelle from their site of synthesis, the cytosol (Hartl and Neupert, 1990). A small number of nuclear-encoded general chaperones, exemplified by Hsp70/DnaK homologs and Hsp60-Hsp10/GroE homologs, assist in import, folding, and solubilization of many different unfolded substrates (Neupert, 1997; Voos and Rottgers, 2002). Specialized chaperones and proteases assist in assembly of specific complexes, for example mitochondrial ribosomes (Nolden et al., 2005) and respiratory chain components (Nijtmans et al., 2000). The protein-folding environment in the mitochondria can be perturbed by malfunction of any of the above components, but also by the expression of a misfolding-prone matrix protein (Zhao et al., 2002) and even by global compromise in expression of the mitochondrial genome (the *rho*$^{-}$ state), which leads to accumulation of unassembled imported subunits (Martinus et al., 1996). Such perturbations selectively induce nuclear genes encoding general mitochondrial matrix chaperones (Hsp70 and Hsp60) and suggest the existence of a mitochondrial unfolded protein response (UPR^{mt}) (Zhao et al., 2002).

We have developed *C. elegans* strains that report on the activity of the UPR^{mt} with integrated green fluorescent protein (GFP) genes driven by the regulatory portions of mitochondrial Hsp60 and Hsp70 genes (*hsp-60$_{pr}$::gfp* and *hsp-6$_{pr}$::gfp*) and confirmed the selectivity of these reporters to mitochondrial unfolded protein stress

(Yoneda et al., 2004). These reporter strains were then applied to a systematic search for genes involved in signaling the UPR^{mt}. A pilot screen of 2445 genes on *C. elegans* chromosome *I* validated the methodology and led to the identification of one gene, *ubl-5*, implicated in a downstream nuclear event in the UPR^{mt} (Benedetti et al., 2006). Having completed a genome-wide screen for genes that signal the UPR^{mt}, we report here on the identification of a pathway extending from the mitochondrial matrix to the nucleus. Interestingly, our observations are consistent with functional conservation of an upstream component of the bacterial heat-shock response in the UPR^{mt}.

RESULTS

A Genome-Wide Screen for Genes Involved in the UPR^{mt}

To identify genes whose inactivation impedes the UPR^{mt}, we made use of a previously characterized worm strain bearing a temperature-sensitive mutation, zc32 *II*, that causes mitochondrial unfolded protein stress and activates the UPR^{mt} at the nonpermissive temperature (Benedetti et al., 2006). Mutant *zc32* worms were fed bacteria from clones individually expressing RNAi constructs directed to 16,757 known *C. elegans* genes (covering ~85% of the protein-coding genes in that species), and the effect of each RNAi clone on expression of an *hsp-60$_{pr}$::gfp* reporter was assessed by fluorescent microscopy of animals at the nonpermissive temperature. The screen was designed to explore the RNAi effect at different levels of exposure and thereby also allowed us to score phenotypes associated with partial inactivation of essential genes (Benedetti et al., 2006).

RNAi clones that interfered with *hsp-60$_{pr}$::gfp* induction and then on retesting with *hsp-6$_{pr}$::gfp* induction were considered candidates for encoding proteins that function in the UPR^{mt}. To select against RNAi clones that interfered with stress responses nonspecifically, we analyzed the candidates for their effect on the UPR^{er} by following *hsp-4$_{pr}$::gfp* induction in ER stressed worms (Yoneda et al., 2004). As a functional UPR^{mt} is predicted to promote survival of stressed animals, the RNAi clones that passed these specificity criteria were tested for their ability to selectively diminish the fitness of animals experiencing unusually high levels of mitochondrial stress imposed by the *zc32* mutation or by high-level expression of GFP in the mitochondria, criteria that have been previously validated (Benedetti et al., 2006).

Of the 16,757 RNAi clones examined, only four passed these criteria (see Tables S1 and S2 in the Supplemental Data available with this article online). The relationships between three of these—*ZK1193.5*, encoding a putative homeobox transcription factor; *ubl-5 (F46F11.4)*, encoding a ubiquitin-like protein; and *ZK970.2*, encoding a protease homologous to bacterial ClpP—will be described in further detail below. The fourth gene, *F54C8.5*, encodes a GTPase homologous to mammalian Rheb and will not be described in detail here.

We turned our attention first to *ZK1193.5*, which encodes a predicted 468 amino acid protein that shares homology with the product of *D. melanogaster dve* (defective proventriculus, Nakagoshi et al., 1998) and mammalian SatB2 (Dobreva et al., 2003) and will be referred to henceforth as *dve-1*. Knockout of *dve-1* is lethal (see below), but partial inactivation by *dve-1*(RNAi) inhibited *hsp-60$_{pr}$::gfp* expression in *zc32* mutant adults at the nonpermissive temperature. Inhibition was observed using RNAi clones that target the transcribed genomic region (Figure 1A) or the 3′ UTR (Figure S1). d*ve-1*(RNAi) also interfered with *hsp-60$_{pr}$::gfp* expression in animals exposed to other conditions that cause mitochondrial unfolded protein stress, such as culture on plates containing ethidium bromide, which leads to imbalanced synthesis of nuclear and mitochondrial encoded proteins and *spg-7*(RNAi), which blocks an essential mitochondrial protease (Yoneda et al., 2004; Nolden et al., 2005; Figure 1B). Specificity for the UPR^{mt} is revealed by the observation that *dve-1*(RNAi) did not affect the upregulation of a UPR^{er} reporter (*hsp-4$_{pr}$::gfp*) by tunicamycin (Figure 1A). Inhibition of the UPR^{mt} reporters was mirrored by the effects of *dve-1*(RNAi) on the expression of the endogenous mitochondrial chaperone genes, *hsp-60* and *hsp-6* (Figure 1C).

DVE-1 Is Required for Embryonic Development and Maintenance of Mitochondrial Morphology

Immunostaining of embryos with antiserum raised to bacterially expressed DVE-1 revealed a signal that colocalized with the DNA-binding dye Hoechst H33258 (Figure 2A), indicating nuclear localization of the endogenous protein. Most cells had some DVE-1 staining, but the strongest signal was observed in the mitochondria-rich intestinal precursor cells. The validity of the anti-DVE-1 staining is supported by the diminished signal in embryos born to *dve-1*(RNAi) mothers and by its concordance with the fluorescent signal in embryos expressing a *dve-1::gfp* transgene controlled by the endogenous promoter (*dve-1$_{pr}$::dve-1::gfp*) (Figure 2A). The *dve-1$_{pr}$::dve-1::gfp* transgene is at least partially functional, as it is able to rescue *dve-1* knockdown by RNAi directed to the gene's 3′UTR (Figure S1), but it is unable to rescue the lethality associated with a null mutation (data not shown).

Heterozygous animals with a deletion allele in *dve-1*(*tm259*)*X* were obtained from the National Bioresource Project for *C. elegans* (Tokyo). The 984 base pair deletion includes exons seven and eight, which encode the predicted DNA-binding domain of DVE-1 and therefore severely disrupts gene function. Homozygous *dve-1*(*tm259*)*X* mutant animals develop normally until ~330 min postfertilization, after which they arrest and degenerate (Figure 2B). Though morphologically normal at this early stage of development, homozygous *dve-1*(*tm259*)*X* mutant embryos born to *spg-7*(RNAi) mothers have attenuated *hsp-60$_{pr}$::gfp* expression, whereas wild-type embryos from *spg-7*(RNAi) mothers express higher levels of *hsp-60$_{pr}$::gfp* (Figure 2C). These findings indicate that activation of the UPR^{mt} in early embryos depends on endogenous *dve-1*.

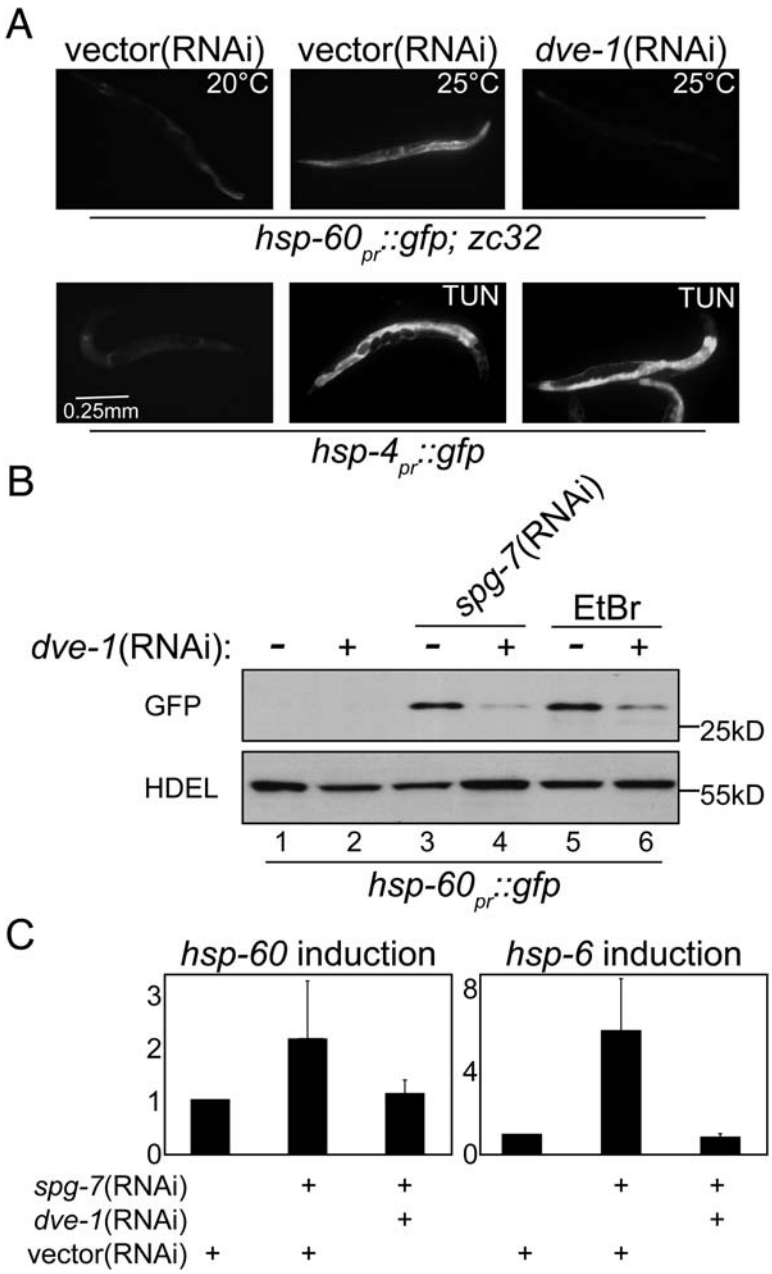

Figure 1. *dve-1* Knockdown Attenuates the UPR^{mt}

(A) Representative fluorescent photomicrographs of *hsp-60$_{pr}$::gfp* transgenic worms (reporting on the UPR^{mt}) with a temperature-sensitive mutation (*zc32*, that activates the UPR^{mt}) raised at the permissive (20°C) or non-permissive temperature (25°C). The lower panels are representative fluorescent photomicrographs of *hsp-4$_{pr}$::gfp* transgenic worms (reporting on the UPR^{er}) following exposure to the ER stress-inducing drug tunicamycin. Where indicated, the animals were exposed to mock (vector) RNAi or to *dve-1*(RNAi).

(B) Immunoblot of GFP expressed by *hsp-60$_{pr}$::gfp* transgenic worms in whom mitochondrial unfolded protein stress was induced by *spg-7*(RNAi) or cultured in the presence of ethidium bromide (EtBr). Where indicated, the animals were subjected to *dve-1*(RNAi). The endogenous ~55 kDa ER protein, detected with an anti-HDEL monoclonal antibody (lower panel), serves as a loading control.

(C) Quantitative analysis (by QRT-PCR, mean ± SEM) of endogenous *hsp-60* and endogenous *hsp-6* mRNA in wild-type animals and in animals subjected to *spg-7*(RNAi) alone or in combination with *dve-1*(RNAi).

To further examine *dve-1*'s effect on mitochondria, we compared the staining pattern of MitoTracker, a mitochondrial vital dye, in wild-type embryos and early *dve-1*(*tm259*)*X* mutant embryos, following an established protocol (Jagasia et al., 2005). In wild-type embryos, MitoTracker staining was most conspicuous in a reticular network surrounding the large DVE-1-positive nuclei of the intestinal precursor cells, whereas staining in the mutant embryos was consistently diminished by 50% (Figure 2D). As MitoTracker is a vital dye taken up actively by the organelle, these observations are consistent with reduced mitochondrial mass, defective membrane potential, or both. To expand on these observations, we sought a marker for mitochondrial mass. A ligand blot assay with a peroxidase-tagged avidin probe identifies a single major species of ~75 kDa in worm lysates that is enriched in the mitochondrial fraction and probably corresponds to the biotinylated mitochondrial enzyme propionyl-CoA carboxylase (Figure S2; Benedetti et al., 2006). Histochemical analysis of fixed embryos with FITC-conjugated avidin reveals a signal that largely overlaps MitoTracker in *dve-1*/+ embryos (Figure S2) and is reduced 55% in *dve-1*(*tm259*)*X* mutant embryos (Figure 2E). These observations are consistent with reduced mitochondrial mass, possibly compounded by a functional defect in the mitochondria of the mutant embryos.

Unmitigated unfolded protein stress compromises mitochondrial morphology, which is readily visualized in

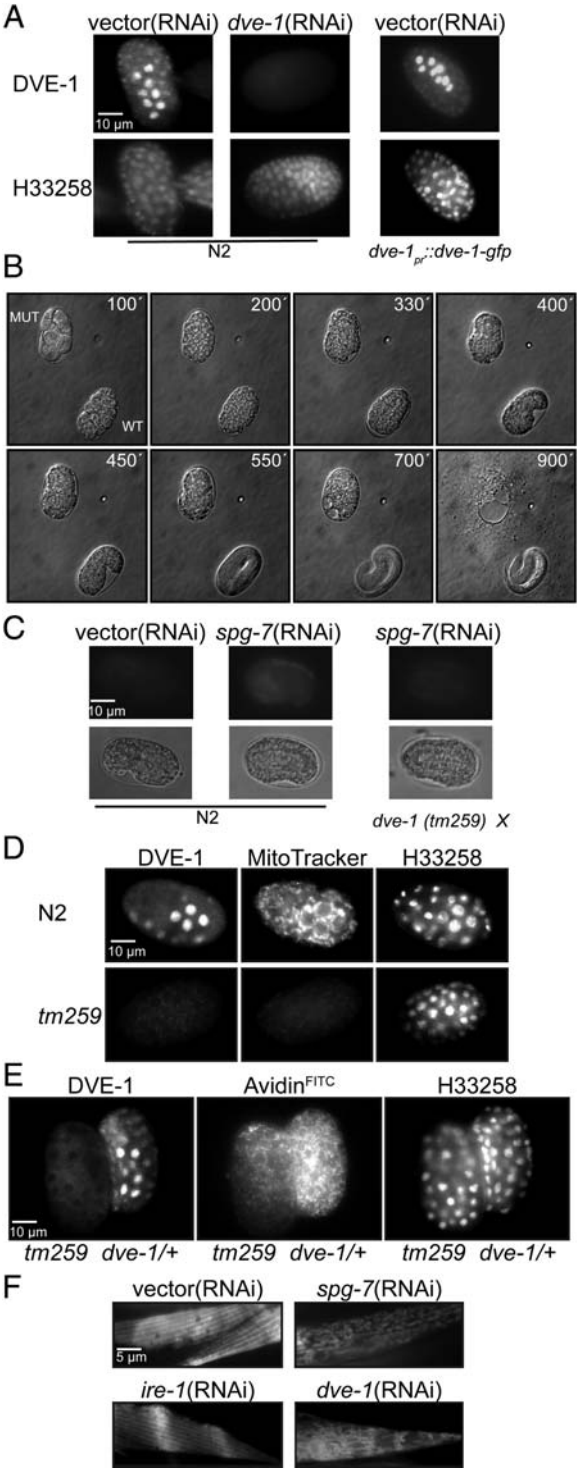

Figure 2. *dve-1* Encodes a Nuclear Protein Essential for Maintenance of Mitochondrial Mass and Morphology

(A) Fluorescent photomicrographs of wild-type and *dve-1*(RNAi) embryos immunostained with antiserum to DVE-1 (left panels) and a similarly staged wild-type embryo bearing a *dve-1*$_{pr}$*::dve-1::gfp* transgene (right panel). The embryos were counterstained with the DNA-binding dye H33258, revealing the nuclear morphology (lower panels).

(B) A time-lapsed series of images of a *dve-1*/+ embryo (lower right) and a sibling *dve-1(tm259)X* mutant embryo (upper left) photographed under phase contrast microscopy.

(C) Fluorescent photomicrographs of wild-type (N2) and *dve-1(tm259)X* mutant embryos transgenic for the UPR^{mt} reporter *hsp-60*$_{pr}$*::gfp* (SJ4203). Where indicated, the animals were subjected to *spg-7*(RNAi).

(D) Fluorescent photomicrographs of wild-type and *dve-1(tm259)X* mutant embryos immunostained for DVE-1 and costained with MitoTracker and H33258.

(E) Fluorescent photomicrographs of the DVE-1 immunostain, Avidin^{FITC} stain, and H33258 labeling of sibling wild-type (*dve-1*/+, on right) and mutant embryos (*tm259*, left).

(F) Fluorescent photomicrographs of body wall muscles of animals transgenic for a mitochondrially localized GFP reporter (*myo-3*$_{pr}$*::GFP*^{mt}). Where indicated, the animals were subjected to inactivation of *spg-7*, known to induce mitochondrial unfolded protein stress, *ire-1*, a negative control that induces ER stress and *dve-1*.

the body wall muscle cells of transgenic animals expressing mitochondrially imported GFP (Labrousse et al., 1999). As noted previously, the fine striated pattern of mitochondria in vector (control) RNAi animals was disrupted by induction of mitochondrial unfolded protein stress by *spg-7*(RNAi) (Benedetti et al., 2006; Figure 2F). A similar perturbation of mitochondrial morphology was also apparent in *dve-1*(RNAi) animals (Figure 2F). These observations are consistent with a mitochondrial perturbation caused by elevated levels of unfolded protein stress in the *dve-1*(RNAi) animals with a compromised UPR^{mt}.

A Stress-Induced Alteration of DVE-1's Nuclear Distribution Correlates with Binding to Mitochondrial Chaperone Genes

Adults transgenic for the *dve-1*$_{pr}$*::dve-1::gfp* reporter normally exhibited bright staining of several head and tail nuclei and a diffuse fluorescence in the intestine. Induction of mitochondrial unfolded protein stress with *spg-7*(RNAi) resulted in the appearance of bright nuclear GFP puncta in the intestine (Figure 3A). These were not associated with a detectable change in global DVE-1::GFP fusion protein levels (Figure 3B). Due to their thick cuticle, we are unable to reliably immunostain adult animals; however, the tissue distribution of these stress-induced changes in DVE-1::GFP localization mirrored the induction of the UPR^{mt} marker *hsp-60*$_{pr}$*::gfp* (Figure 3C), supporting its physiological relevance. Activity-dependent changes in nuclear localization have also been noted in DVE-1's mammalian homologs, SATB1 and SATB2 (Cai et al., 2003; Dobreva et al., 2003), but the relationship of those findings to ours remains unknown.

Chromatin immunoprecipitation of DVE-1::GFP complexes with our anti-GFP serum was plagued by high background. Therefore, we created a transgenic line in which DVE-1 is tagged by Myc$_3$-His$_6$. In these *dve-1*$_{pr}$*::dve-1*^{TAG} transgenic animals, the endogenous *hsp-60* and *hsp-6* promoter fragments were selectively recovered in complex with the tagged protein on Ni^{+} agarose beads (Figure 3D). However, promoter binding was not reproducibly increased by induction of mitochondrial unfolded protein stress (data not shown), suggesting that

overexpression deregulates aspects of DVE-1 function. We were unable to reliably detect the endogenous mitochondrial chaperone promoters in complex with endogenous DVE-1, even in stressed animals; however, the endogenous protein was immunoprecipitated in a specific complex with the promoter of the *hsp-60*$_{pr}$*::gfp* transgene (the *hsp-60* promoter is likely present at high copy number in the integrated array, increasing signal strength). Importantly, the latter complex was increased by mitochondrial unfolded protein stress in mutant *zc32* animals (Figure 3E). These observations correlate activation of the UPR^{mt} with binding of DVE-1 to mitochondrial chaperone genes.

A Complex between UBL-5 and DVE-1 in Stressed Animals

RNAi of the gene encoding the ubiquitin-like protein, UBL-5, blocks the UPR^{mt} (Benedetti et al., 2006; Figure 4A). As a substantial fraction of UBL-5 is found in the nucleus of mitochondrially stressed worms (Benedetti et al., 2006), we hypothesized that it might collaborate with DVE-1 in activating the UPR^{mt}. A transgenic line expressing Myc_3-His_6-tagged UBL-5 (^{TAG}UBL-5) and DVE-1::GFP, both under the control of their endogenous promoters, was created. When subjected to mitochondrial stress by *spg-7*(RNAi), DVE-1::GFP was recovered in complex with ^{TAG}UBL-5 (Figure 4B). Complex formation appears to be regulated at the level of UBL-5 expression, whose levels increase in the stressed animals (Benedetti et al., 2006; Figure 4B, input panel), a point to be addressed in more detail below.

Mitochondrial stress was also associated with the formation of a complex between ^{TAG}UBL-5 and the endogenous DVE-1 protein (Figure 4C), and in mammalian cells, too, a tagged mammalian homolog of DVE-1 (FLAG-SATB2) formed a complex with GST-tagged mammalian UBL5 (Figure 4D). Only ~1% of the total tagged DVE-1 is recovered in complex with tagged UBL-5 in these coprecipitation experiments, which may attest to the complex's lability; all the same, these observations suggest a conserved physical interaction between the products of two genes implicated in the *C. elegans* UPR^{mt}.

A *C. elegans* ClpP Homolog Required for UPR^{mt} Signaling and DVE-1 Activation

The third gene identified in our screen, *ZK970.2*, encodes a 221 amino acid protein homologous to the bacterial protease ClpP, which we refer to as *clpp-1*. Like *dve-1*(RNAi) and *ubl-5*(RNAi), *clpp-1*(RNAi) interferes with *hsp-60*$_{pr}$*::gfp* induction by mitochondrial stress (Figure 5A). Like *dve-1*(RNAi) and *ubl-5*(RNAi), *clpp-1*(RNAi) also perturbed mitochondrial morphology (Figure 5B), a finding consistent with higher levels of unfolded protein stress in the organelle of animals lacking CLPP-1.

The major difference between CLPP-1 and bacterial ClpP is an N-terminal extension of the *C. elegans* protein, suggestive of a mitochondrial targeting sequence. Transgenic lines expressing wild-type and N-terminally deleted (ΔSS), C-terminally tagged CLPP-1 driven by a heat-shock inducible promoter (*hsp-16*$_{pr}$*::clpp-1*^{WT}*::TAG* and *hsp-16*$_{pr}$*::clpp-1*$^{\Delta SS}$*::TAG*) were created. The wild-type protein, expressed by the *hsp-16*$_{pr}$*::clpp-1*^{WT}*::TAG* transgene, was enriched in the mitochondrial fraction, whereas the mutant lacking the N-terminal extension was predominantly cytosolic (Figure 5C). Furthermore, CLPP-1 recovered in mitoplasts was protected from protease digestion (Figure S3), consistent with localization to the mitochondrial matrix. Velocity gradient centrifugation showed that CLPP-1^{WT}::TAG was present in a large complex consistent in size with a homo-oligomer of 14 subunits (Figure 5D), like its bacterial homolog (Sauer et al., 2004).

The observations above suggest that CLPP-1 localizes to the mitochondrial matrix, where it forms a high-molecular-weight complex implicated in mitochondrial chaperone induction. As the latter is a nuclear process, we hypothesized that CLPP-1 might function upstream of DVE-1 and UBL-5.

First, we assessed the effect of *clpp-1* inactivation on the localization of DVE-1::GFP in stressed animals. RNAi of *clpp-1* inhibited the redistribution of DVE-1::GFP to nuclear puncta in *zc32* mutant animals at the nonpermissive temperature (Figure 6A), without affecting the quantity of DVE-1::GFP protein in the animals (Figure 6D). Consistent with these observations, *clpp-1*(RNAi) also prevented DVE-1 from binding to the *hsp-60* promoter in mitochondrially stressed animals. By contrast, *ubl-5*(RNAi), which also inhibits the UPR^{mt}, had no consistent effect on puncta formation or promoter binding (Figures 6A and 6B).

Next, we assessed the effect of *clpp-1*(RNAi) on the induction of *ubl-5* by mitochondrial misfolded protein stress. Inactivation of *spg-7* markedly increased reporter activity of *ubl-5*$_{pr}$*::gfp* transgenic worms, as predicted (Benedetti et al., 2006). Coincidental *clpp-1*(RNAi) attenuated the induction of *ubl-5*$_{pr}$*::gfp* by *spg-7*(RNAi) (Figure 6C) and resulted in lower levels of tagged UBL-5 in *ubl-5*$_{pr}$*::*^{TAG}*ubl-5* transgenic animals (Figure 6D). As expected, the *clpp-1*(RNAi)-attenuated expression of *ubl-5* resulted in lower levels of ^{TAG}UBL-5+DVE-1::GFP complex formation (Figure 6D). These observations place *clpp-1* upstream of *ubl-5* induction and DVE-1 relocalization in mitochondrially stressed animals. We further noted that whereas *dve-1*(RNAi) reproducibly attenuated *ubl-5* activation, *ubl-5*(RNAi) had no similar inhibitory effect (Figure 6C). The implications of these findings for the epistatic relationship of the three genes will be discussed below.

In our experimental system, activation of mitochondrial chaperone genes required sustained perturbation of mitochondrial protein-folding homeostasis over the 3 days of worm development; manipulation of the fully developed adult animal had at most a very minor effect on *hsp-60*$_{pr}$*::gfp* expression (data not shown). However, we noted that shifting fully developed adult *ubl-5*$_{pr}$*::gfp* transgenic animals to elevated temperature led to induction of the reporter gene within 3 hr (Figure 7A). This induction was unaffected by *hsf-1*(RNAi), which potently inhibits the UPR^{cyt} reporter *hsp-1*$_{pr}$*::gfp* (Figure S4), but was strongly attenuated by *clpp-1*(RNAi) and to a lesser extent by *dve-1*(RNAi) (Figure 7A).

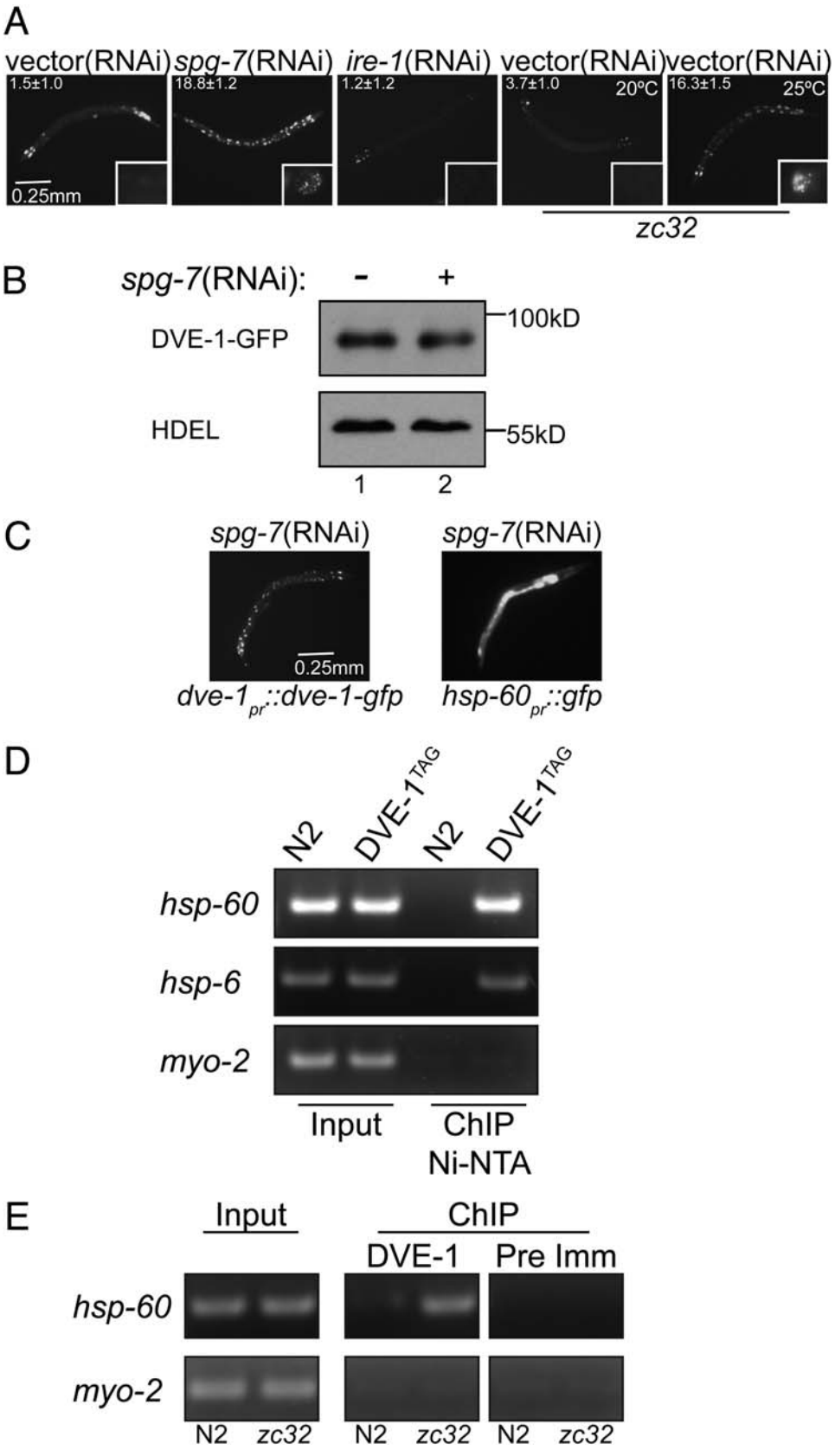
A
vector(RNAi)
spg-7(RNAi)
ire-1(RNAi)
vector(RNAi)
vector(RNAi)
1.5±1.0
18.8±1.2
1.2±1.2
3.7±1.0
20ºC
16.3±1.5
25ºC
0.25mm
zc32
B
spg-7(RNAi): - +
DVE-1-GFP
100kD
HDEL
55kD
1 2
C
spg-7(RNAi)
spg-7(RNAi)
0.25mm
dve-1pr::dve-1-gfp
hsp-60pr::gfp
D
N2
DVE-1TAG
N2
DVE-1TAG
hsp-60
hsp-6
myo-2
Input
ChIP
Ni-NTA
E
Input
ChIP
DVE-1
Pre Imm
hsp-60
myo-2
N2 zc32 N2 zc32 N2 zc32

The above observations suggested a role for *clpp-1* in signaling the consequences of a rapidly developing mitochondrial perturbation (by elevated temperature) to the nucleus. The relatively short latency of this *clpp-1*-dependent response suggested a way to distinguish between a developmental role for *clpp-1* in establishing conditions for the signaling pathway to exist and a more direct role for CLPP-1-mediated proteolysis in signaling itself. We confirmed that the *E. coli* ClpP inhibitor Z-LY-CMK (Szyk and Maurizi, 2006) and the peptide aldehyde MG132 (a known proteasome inhibitor) attenuate hydrolysis of a reporter substrate, SUC-LLVY-AMC, by CLPP-1^{WT}::TAG purified from worms (Figure 7B). Injection of either inhibitor into young adult *ubl-5$_{pr}$::gfp* transgenic worms attenuated reporter gene expression in response to elevated temperature: At 30°C, the average *ubl-5$_{pr}$::gfp* signal of Z-LY-CMK-injected animals was 2 ± 1.24, 2.75 ± 1.035 in MG132-injected animals and 5.0 ± 0 in animals injected with the carrier DMSO solvent (mean ± SD, using a semiquantitative visual scale for intestinal GFP fluorescence; see Experimental Procedures) (Figure 7C). Proteasomal inhibition is unlikely to account for this effect, as *pas-6*(RNAi), which encodes a subunit of the 20S proteasome, did not attenuate *ubl-5$_{pr}$::gfp* induction at elevated temperature. Neither Z-LY-CMK nor MG132 injection blocked induction of *aip-1$_{pr}$::gfp* by arsenite, controlling for the potential toxicity of short-term exposure to these protease inhibitors (Figure 7C, lower panels). While we cannot exclude the possibility that the inhibitors are exerting their effect on the UPR^{mt} by inhibiting enzymes other than CLPP-1, these observations are consistent with a direct role for CLPP-1-mediated proteolysis in signaling from stressed mitochondria to the nucleus.

DISCUSSION

This paper reports on a genome-wide analysis of a signaling pathway linking perturbation of the protein-folding environment in the mitochondrial matrix to expression of nuclear encoded mitochondrial chaperone genes. We have chosen to study the UPR^{mt} in *C. elegans* because of the ease with which the response can be elicited by genetic manipulation of the folding environment in the mitochondria (Yoneda et al., 2004). Stringent criteria were applied to eliminate genes whose inactivation suppressed the expression of mitochondrial chaperones indirectly. Consequently, the effort yielded four genes, three of which can be plausibly ordered in a pathway stretching from the mitochondrial matrix to the promoters of the UPR^{mt}'s targets in the nucleus.

An important finding concerns *dve-1*, whose inactivation interferes with UPR^{mt} target gene expression. The encoded protein, which contains a predicted DNA-binding domain related to the homeobox, is nuclear and can be crosslinked to the promoters of UPR^{mt} target genes in stressed *C. elegans*. Furthermore, the nuclear distribution of DVE-1 is altered by application of mitochondrial stress. These observations favor a simple model whereby DVE-1 binds and activates mitochondrial chaperone genes in stressed cells.

In stressed worms, a DVE-1::GFP fusion protein (expressed from the endogenous promoter) forms a complex with the small ubiquitin-like protein, UBL-5 (tagged and expressed from its endogenous promoter). UBL-5 is the product of another gene identified by this screen as both a transcriptional target of the UPR^{mt} and as a gene required for development of the full response. As both proteins reside outside the mitochondria, formation of a complex between endogenous DVE-1 and UBL-5 (assuming it occurs) is likely to be important in a relatively downstream step of the UPR^{mt}. Our data suggest that CLPP-1, the *C. elegans* homolog of the bacterial ClpP protease, functions upstream in the UPR^{mt}, as *clpp-1*(RNAi) prevents both the redistribution of DVE-1 to nuclear puncta and the induction of *ubl-5*. An upstream role for CLPP-1 is consistent with its location in the mitochondrial matrix where, presumably, the stress signal originates. The proposed epistatic relationships between *clpp-1*, *dve-1*, and *ubl-5* are presented in cartoon form in Figure 7D.

The fourth gene identified by our screen encodes a *C. elegans* homolog of Rheb, a GTPase implicated in signaling via TOR, which is a kinase that integrates nutritional and stress cues in eukaryotes (Manning and Cantley, 2003). Inactivation of either this Rheb homolog or *C. elegans* TOR blocks *hsp-60$_{pr}$::gfp* expression in stressed worms but does not interfere with *dve-1* or *ubl-5*. Rather, *rheb-1* inactivation promotes nuclear redistribution of DVE-1, induction of *ubl-5*, and complex formation with

Figure 3. Stress-Induced Alteration of DVE-1 Localization and Association with Promoters of Mitochondrial Chaperone Genes

(A) Fluorescent photomicrographs of adult *dve-1$_{pr}$::dve-1::gfp* wild-type transgenic animals, *spg-7*(RNAi), *ire-1*(RNAi) (a negative control), and *zc32* mutant animals at the permissive (20°C) and nonpermissive (25°C) temperature. The inset in the upper left-hand corner reports on the mean ± SEM number of intestinal cells with puncta per animal and that in the lower right-hand corner is a high-magnification view of an intestinal nucleus.

(B) Immunoblot of the DVE-1::GFP fusion protein in wild-type and *spg-7*(RNAi) *dve-1$_{pr}$::dve-1::gfp* transgenic animals. The anti-HDEL blot (lower panel) serves as a loading control.

(C) Fluorescent photomicrographs of stressed *dve-1$_{pr}$::dve-1::gfp* and *hsp-60$_{pr}$::gfp* transgenic animals showing the increase in mitochondrial chaperone gene expression and redistribution of DVE-1::GFP in the intestine.

(D) Ethidium bromide-stained gel of PCR-amplified promoter regions of the indicated genes. The template for the PCR reaction is the input lysate ("Input") or the material recovered by Ni-NTA purification ("ChIP") from nontransgenic (N2, a negative control) and *dve-1$_{pr}$::dve-1^{TAG}* (DVE-1^{TAG}) transgenic animals.

(E) Ethidium bromide-stained gel of PCR-amplified promoter regions of the *hsp-60$_{pr}$::gfp* transgene (present at high copy number) and endogenous *myo-2* (a negative control). The template for the PCR reaction is the input lysate ("Input") or the material recovered by anti-DVE-1 immunoprecipitation (ChIP, DVE-1) and immunoprecipitation using preimmune serum (ChIP, Pre Imm, a negative control) from wild-type *hsp-60$_{pr}$::gfp* transgenic and stressed *zc32* mutant *hsp-60$_{pr}$::gfp* transgenic animals.

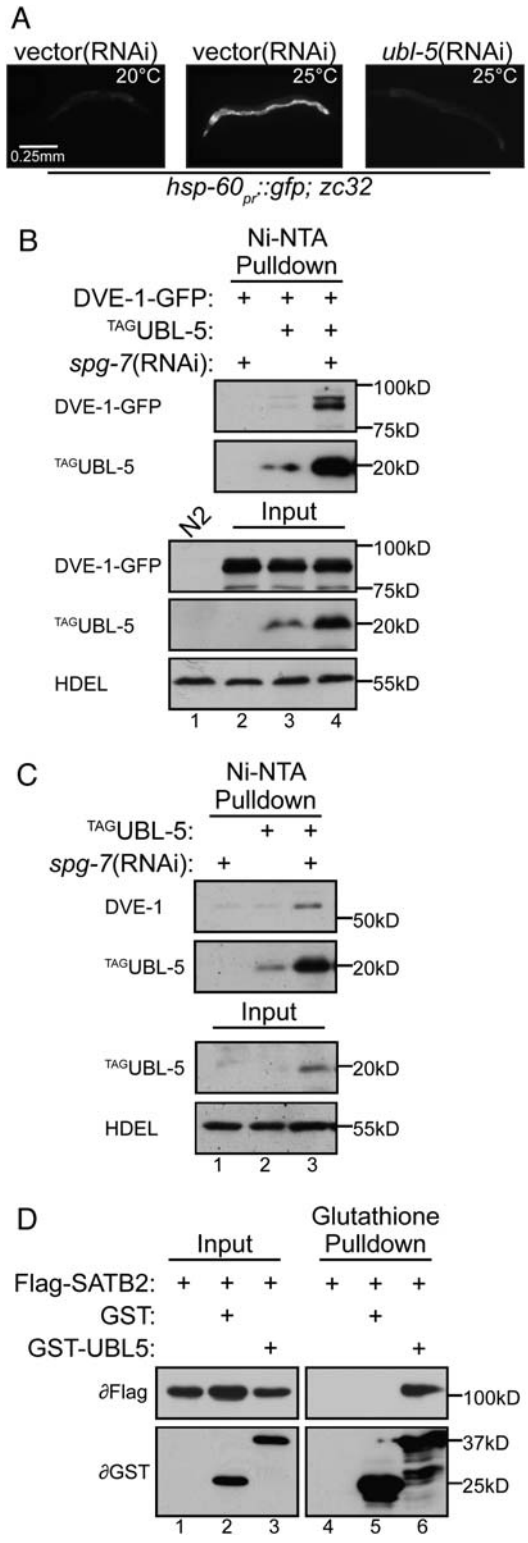

Figure 4. Mitochondrial Stress-Induced Expression of UBL-5 and Complex Formation with DVE-1

(A) Fluorescent photomicrographs of *hsp-60*$_{pr}$*::gfp* transgenic *zc32* mutant animals at the permissive (20°C) and nonpermissive (25°C) temperature. Where indicated, the animals were subjected to *ubl-5*(RNAi).

(B) DVE-1 immunoblots of proteins recovered in complex with tagged UBL-5 by Ni-NTA agarose chromatography from lysates of *dve-1*$_{pr}$*::dve-1::gfp* transgenic worms that lack or have an additional *ubl-5*$_{pr}$*::*^{TAG}*ubl-5* transgene (^{TAG}UBL-5). Where indicated, mitochondrial unfolded protein stress was induced by *spg-7*(RNAi). The anti-Myc blot (lower panel) reports on the amount of ^{TAG}UBL-5 recovered in purification procedure, whereas the panel labeled "Input" reports on protein levels in the worm lysate before purification.

(C) Immunoblot of endogenous DVE-1 recovered in complex with ^{TAG}UBL-5 from unstressed and *spg-7*(RNAi) *ubl-5*$_{pr}$*::*^{TAG}*ubl-5* transgenic animals.

(D) Immunoblot of FLAG epitope-tagged mammalian DVE-1 homolog (SATB2) recovered by glutathione affinity chromatography from lysates of 293T cells cotransfected with FLAG-SATB2 and GST-tagged mouse UBL5 or GST alone (a negative control). The panel labeled "Input" reports on protein levels in the cell lysate before purification.

DVE-1 (data not shown). These observations are consistent with a model whereby *rheb-1* and TOR mediate signaling that feeds back negatively on the pathway defined by *clpp-1*, *dve-1*, and *ubl-5*. It is interesting to note in this regard that inactivation of TOR by rapamycin has recently been shown to decrease *hsp-60* transcript levels in cultured *Drosophila* cells (Guertin et al., 2006).

Both formation of a DVE-1/UBL-5 complex and nuclear redistribution of DVE-1 correlate with activation of the UPR^{mt}. On the *ubl-5* side, it seems that *clpp-1*-dependent transcriptional induction is important. This transcriptional induction is likely to be part of an amplification circuit that operates in the UPR^{mt}, as it is attenuated by *dve-1*(RNAi) (Figures 6C and 7A). We do not know if DVE-1 is a direct activator of *ubl-5* or if its effects are mediated indirectly (e.g., by facilitating mitochondrial biogenesis). DVE-1 redistributes to bright nuclear puncta in response to chronic and acute mitochondrial stress (Figures 3A and 6A and Figure S5). This process, which correlates with promoter binding, is *clpp-1* dependent and *ubl-5* independent, but its basis is otherwise not understood. The nuclear distribution of SATB2, a mammalian homolog of DVE-1, appears to be regulated by SUMO conjugation (Dobreva et al., 2003); however, we were unable to detect modified forms of DVE-1 by immunoblot of stressed or unstressed worm lysates.

In *S. pombe*, inactivation of the *ubl-5* homolog, *HUB1*, leads to accumulation of unspliced pre-mRNAs (Wilkinson et al., 2004), and the lethal phenotype of *HUB1* deletion can be rescued by overexpressing Rpb10, a subunit of RNA polymerase (Yashiroda and Tanaka, 2004). We have not detected accumulation of unspliced mitochondrial chaperone pre-mRNAs in *ubl-5*(RNAi) worms, nor have we observed the pervasive splicing defects predicted by the studies in *S. pombe* (data not shown). Nonetheless, these observations suggest a conserved role for UBL-5 in some nuclear step of gene expression relevant to the UPR^{mt}.

The most intriguing question posed by our findings concerns the role of CLPP-1 in the UPR^{mt}. Bacterial ClpP is involved in the proteolysis of diverse substrates, including defective translation products of mRNA fragments, enzymes, and regulatory factors (Gottesman,

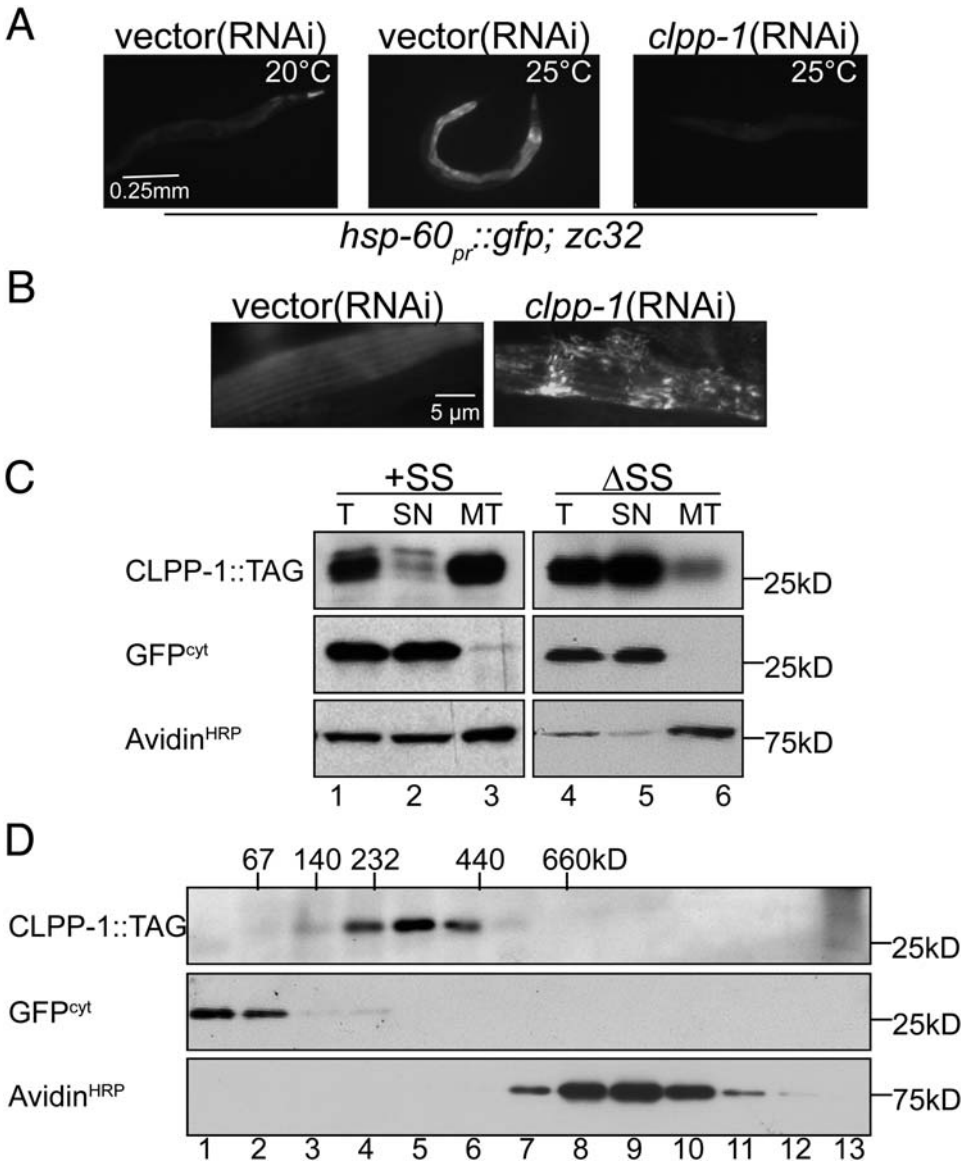

Figure 5. *clpp-1* Encodes a Mitochondrially Localized Homolog of Bacterial ClpP that Is Implicated in the UPR^{mt}

(A) Fluorescent photomicrographs of *hsp-60$_{pr}$::gfp* transgenic *zc32* mutant animals at the permissive (20°C) and nonpermissive (25°C) temperature. Where indicated, the animals were subjected to *clpp-1*(RNAi).

(B) Fluorescent photomicrographs of body wall muscles of wild-type vector (RNAi) and *clpp-1*(RNAi) animals transgenic for a mitochondrially localized GFP reporter (*myo-3$_{pr}$::GFP^{mt}*).

(C) CLPP-1::TAG immunoblot (detected through a C-terminal Myc tag) in total lysate (T), postmitochondrial supernatant (SN), and mitochondrial pellet (MT) of worms expressing transgenic CLPP-1::TAG that either has (+SS) or lacks (ΔSS) the N-terminal mitochondrial targeting sequence . The anti-GFP immunoblot of *myo-3$_{pr}$::GFP^{cyt}* (GFP^{cyt}) and avidin^{HRP} ligand blot serve as cytosolic and mitochondrial markers, respectively. To induce the *hsp-16* promoter-driven expression of CLPP-1::TAG, animals were incubated at 30°C for 3 hr and allowed to recover at 20°C for 4 hr prior to lysis.

(D) Immunoblot of CLPP-1::TAG in fractions of a glycerol gradient loaded with detergent lysate of transgenic *hsp-16$_{pr}$::clpp-1^{WT}::TAG(zcIs21) V* animals. The anti-GFP immunoblot of *myo-3$_{pr}$::GFP^{cyt}* (GFP^{cyt}) is a marker for proteins that do not enter complexes, and the avidin^{HRP} ligand blot serves as a marker for proteins known to form large complexes (~800 kDa).

2003). Therefore, CLPP-1 may contribute to the biogenesis of the UPR^{mt} signaling apparatus. However, our observations are more consistent with a direct role for CLPP-1 proteolysis in the UPR^{mt}, as an inhibitor of its proteolytic activity rapidly blocked signaling when applied to animals that had developed normally up to that point (Figure 7C).

In *E. coli*, ClpP degrades RseA, a repressor of σ^E, the transcription factor activating the extracytoplasmic stress response (Flynn et al., 2004), and in stressed gram-positive bacteria, ClpP degrades CtsR, a labile repressor of the heat-shock response (Kruger et al., 2001). It is possible, therefore, that the degradation of repressors of the

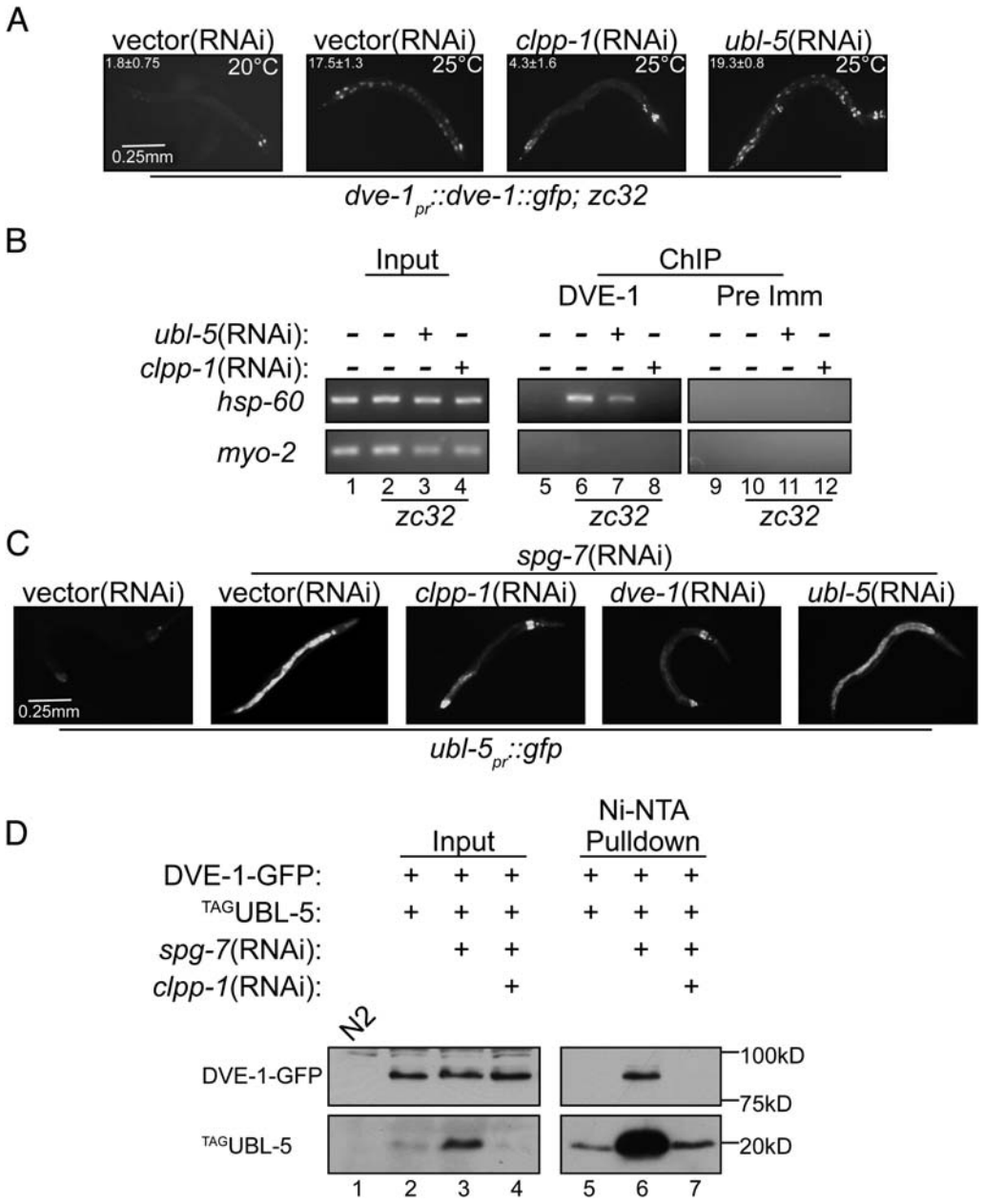

Figure 6. *clpp-1*(RNAi) Interferes with DVE-1 and UBL-5 Activation in the UPR^{mt}

(A) Fluorescent photomicrographs of *zc32 dve-1*$_{pr}$*::dve-1::gfp* transgenic animals grown at the permissive (20°C) or restrictive temperature (25°C) fed vector(RNAi), *clpp-1*(RNAi), or *ubl-5*(RNAi). The inset at the upper left corner reports on the mean ± SEM number of intestinal cells with puncta per animal.

(B) Ethidium bromide-stained gel of PCR-amplified promoter regions of the *hsp-60*$_{pr}$*::gfp* transgene and endogenous *myo-2* (a negative control). The template for the PCR reaction is the input lysate ("Input") or the material recovered by anti-DVE-1 immunoprecipitation (ChIP, DVE-1) from wild-type *hsp-60*$_{pr}$*::gfp* transgenic animals and stressed *zc32* mutant *hsp-60*$_{pr}$*::gfp* transgenic animals exposed to vector (control) RNAi, *clpp-1*(RNAi) or *ubl-5*(RNAi).

(C) Fluorescent photomicrographs of adult *ubl-5*$_{pr}$*::gfp* transgenic animals exposed to *spg-7*(RNAi) without (vector) or in combination with *clpp-1*(RNAi), *dve-1*(RNAi), or *ubl-5*(RNAi).

(D) DVE-1 immunoblots of proteins recovered in complex with tagged UBL-5 by Ni-NTA agarose chromatography from lysates of *dve-1*$_{pr}$*::dve-1::gfp; ubl-5*$_{pr}$*::*^{TAG}*ubl-5* compound transgenic worms subjected to *spg-7*(RNAi) in combination with *clpp-1*(RNAi).

stress response by ClpP/CLPP-1 has been conserved from bacteria to mitochondria. In that case, the mitochondrial substrate(s) of CLPP-1 might no longer resemble their counterparts in the protomitochondrial symbiont (a bacterium), as the latter signal in a compartment topologically equivalent to the mitochondrial matrix whereas

the transcriptional response to mitochondrial stress has been exported across two membranes to the cytosolic/nuclear compartment.

E. coli ClpP associates with two known AAA ATPases, ClpA and ClpX, which are involved in substrate recognition, unfolding, and degradation. *C. elegans* lacks a recognizable homolog of ClpA but has two ClpX homologs (*D2030.2* and *K07A3.3*); interestingly, their inactivation (first separately and then simultaneously) had no effect on *hsp-60$_{pr}$::gfp* or *ubl-5$_{pr}$::gfp* induction (Figure S6; data not shown). In yeast mitochondria, the inner-membrane protein, Mdl1, transports peptides generated by matrix proteases into the cytoplasm (Young et al., 2001). Animal cells have homologous proteins, though their role in peptide transport has yet to be demonstrated. In an alternative, highly speculative model, perturbed protein folding homeostasis in the mitochondria promotes CLPP-1-mediated generation of peptides whose transport into the cytoplasm signals the UPR^{mt}. These observations suggest the existence of hitherto unrecognized ClpP/CLPP-1 adaptors and substrates that function in the UPR^{mt}; their identification is now a high priority.

EXPERIMENTAL PROCEDURES

Transgenic and Mutant *C. elegans* Strains

Strains containing the UPR^{mt} reporters *hsp-6$_{pr}$::gfp(zcIs13) V* and *hsp-60$_{pr}$::gfp(zcIs9) V*, the UPR^{er} reporter *hsp-4 $_{pr}$::gfp(zcIs4) V*, the *zc32 II* mutation that induces the UPR^{mt}, and the expression of cytosolic and mitochondrial GFP *myo-3$_{pr}$::gfp^{cyt}(zcIs21)* and *myo-3$_{pr}$::gfp^{mt}(zcIs14)* have all been previously described (Yoneda et al., 2004; Benedetti et al., 2006).

The *hsp-16$_{pr}$::clpp-1^{WT}::TAG(zcIs21) V* transgene was created by coinjecting plasmids myo-3.gfp and hsp-16.Clpp-1.TAG.V2 into N2 animals generating strain SJ4157. An inducible promoter was used to avoid potential toxicity of constitutive CLPP-1^{WT}::TAG or CLPP-1$^{\Delta SS}$::TAG overexpression. The Myc$_3$-His$_6$ TAG was PCR amplified from pJF105 (a gift from Julia Flynn and Tania Baker) and ligated into pPD49.83, creating plasmid hsp-16.Tag.V1. The entire *clpp-1* coding sequence was PCR amplified from cDNA and ligated 3′ of the *hsp-16* promoter in frame with the Myc$_3$-His$_6$ tag creating plasmid hsp-16.Clpp-1.TAG.V2. CLPP-1$^{\Delta SS}$::TAG (SJ4202) was obtained by PCR from cDNA using primers that excluded the first 45 nucleotides of the CLPP-1 coding sequence, leading to initiation at the second AUG codon.

The strain expressing DVE-1 fused to GFP at its C-terminal residue 468 (SJ4197) was generated by injecting N2 animals with the plasmid dve-1.DVE-1.GFP integrated as *dve-1$_{pr}$::dve-1::gfp(zcIs39) II*. This is a minigene with the DVE-1 coding sequence derived from cDNA fused to GFP, and its expression is driven by a genomic fragment extending 2295 nucleotides upstream of the *dve-1* start codon and fused to the cDNA at exon 2. The strain expressing DVE-1 fused at the C terminus to a Myc$_3$-His$_6$ tag was generated by coinjecting plasmids dve-1.DVE-1.TAG and myo-3.gfp into N2 animals integrated as *dve-1$_{pr}$::dve-1^{TAG} (zcIs40) X* in strain SJ4199. The plasmid dve-1.DVE.TAG is identical to dve-1.DVE-1.GFP with the exception that GFP is replaced with Myc$_3$-His$_6$. The allele *ubl-5$_{pr}$::^{TAG}ubl-5 (zcIs41) V* was created by coinjecting plasmids myo-3.gfp and ubl-5.H6Myc.ubl-5 into N2 animals. Strain SJ4200 expresses UBL-5 tagged at the N termini with the Myc$_3$-His$_6$ tag driven by the *ubl-5* promoter. The plasmid ubl-5.H6Myc.ubl-5 consists of the *ubl-5* promoter (nucleotides −780 to −12 relative to the start codon) followed by the Myc$_3$-His$_6$ tag fused in frame with the start codon of *ubl-5* derived from cDNA. Three identically behaving independently derived *ubl-5$_{pr}$::gfp* lines were created by injecting the plasmid ubl-5.gfp consisting of the above promoter fragment driving GFP expression.

Screening and RNAi Procedures

Systematic inactivation of genes on *C. elegans* chromosomes *II*, *III*, *IV*, *V*, and *X* was conducted as previously described (Benedetti et al., 2006). In brief, four L4 larvae of the *zc32 II*; *hsp-60$_{pr}$::gfp(zcIs9) V* genotype were placed on plates seeded with *E. coli* expressing double-stranded RNA of a specific gene (Kamath et al., 2003). Their progeny were allowed to develop for 36 hr at the permissive temperature (20°C) and then shifted to the nonpermissive temperature (25°C) and observed 48–72 hr later. At this point, the plate was populated with F1 progeny presenting a spectrum of levels of gene knockdown.

The inserts of the RNAi clones that passed our selection criteria were sequenced, and the RNAi phenotype of the clone from the genomic library was confirmed by constructing cDNA-based RNAi feeding plasmids: CLPP-1.cDNA.RNAi was created by inserting a fragment corresponding to nucleotides 133–621 of the cDNA into pPD129.36, DVE-1.3′UTR.RNAi was created by inserting the 522 nucleotide fragment 65 nucleotides downstream of the stop codon in the *dve-1* cDNA into pPD129.36, and the *ubl-5* cDNA feeding plasmids were previously described (Benedetti et al., 2006).

Immunostaining, Microscopy, and Image Analysis

Treatment of worms with ethidium bromide and tunicamycin was described previously (Yoneda et al., 2004). MitoTracker Red CMXROS (Molecular Probes) staining was performed by placing animals on plates containing 2 μg/ml and grown for at least 24 hr. For immunostaining, animals were grown on the appropriate RNAi plate, washed off, and bleached to isolate embryos. The embryos were then fixed, freeze cracked, and immunostained as described (Fukushige et al., 2006). Avidin^{Fitc} (Jackson Laboratories) staining was performed by incubating embryos in a 1:200 dilution for 1 hr at 4°C.

Antibodies, Immunoprecipitation, Immunoblots, and Ligand Blot

Polyclonal serum was raised in rabbit by immunization with a fragment of DVE-1 (26–468), expressed as a His$_6$-tagged fusion protein in *E. coli*. Crude serum was used in immunoblots at a dilution of 1:8000. To immunostain embryos, the serum was cleared of reactivity to common bacterial antigens by passage through an affinity column made of soluble *E. coli* proteins coupled to sepharose.

Compound transgenic worms were homogenized in 50 mM NaH_2PO_4, 300 mM NaCl, 1% Triton X-100, and 10 mM imidazole (pH 8.0), and proteins were purified by Ni-NTA affinity chromatography and detected by immunoblotting with antisera to GFP, Myc (9E10), or DVE-1. An endogenous ER protein reactive with a monoclonal antibody to the peptide NH2-HDEL-COOH ("HDEL") and endogenous biotinylated mitochondrial proteins were detected with HRP-conjugated avidin by ligand blot, as described (Benedetti et al., 2006). Likewise, analysis of CLPP-1-containing complexes by velocity gradient centrifugation was performed on a 10%–40% glycerol gradient as previously described (Benedetti et al., 2006).

N-terminally FLAG-epitope-tagged mouse SATB2 and GST-tagged mouse UBL5 were coexpressed in 293T cells from the plasmids pEF-Flag-SATB2 (Dobreva et al., 2003) and mUBL5.pEBG.V1 (consisting of a fusion of GST and mouse UBL5 at the first amino acid) and purified by glutathione affinity chromatography, and the proteins were detected by immunoblot using the FLAG-M2 monoclonal antibody (Sigma) and polyclonal serum to GST.

ChIP Experiments and Quantitative PCR

Chromatin immunoprecipitation from formaldehyde-fixed worm lysates was performed following a published protocol (Oh et al., 2006). Animals were treated with bleach to synchronize the population and grown in liquid with the appropriate RNAi for 72 hr. Approximately 250 mg of worms was recovered by sucrose flotation, followed by fixation in 1% formaldehyde for 1 hr. The reaction was quenched by

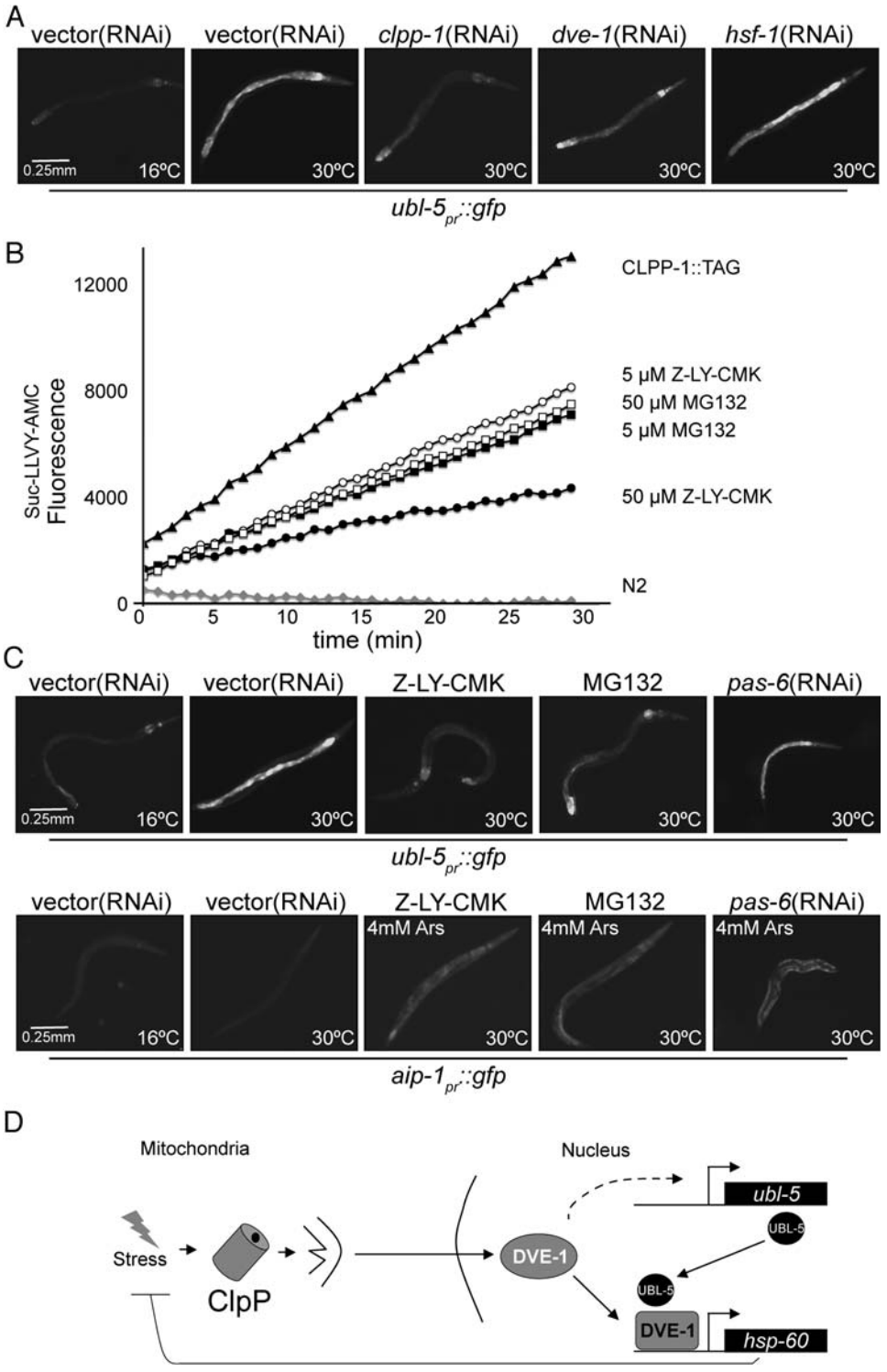

Figure 7. Induction of UBL-5 Is Dependent on CLPP-1 Proteolytic Activity

(A) Fluorescent photomicrographs of young adult *ubl-5*$_{pr}$*::gfp* transgenic animals raised at 16°C and incubated at 30°C for 6 hr to induce mitochondrial stress. Where indicated, the animals were subjected to *clpp-1*(RNAi), *dve-1*(RNAi), or *hsf-1*(RNAi).

(B) Digestion of the fluorogenic peptide suc-LLVY-AMC by immunopurified CLPP-1::TAG. Where indicated, the inhibitors Z-LY-CMK and MG132 were added prior to addition of suc-LLVY-AMC.

(C) Fluorescent photomicrographs of young adult *ubl-5*$_{pr}$*::gfp* or *aip-1*$_{pr}$*::gfp* transgenic animals raised at 16°C, microinjected with DMSO (control), Z-LY-CMK, or MG132 and incubated at 30°C for 6 hr to cause mitochondrial stress. Arsenic-inducible reporter *aip-1*$_{pr}$*::gfp* animals (Stanhill et al.,

adding 0.125 M glycine followed by resuspension in lysis buffer (Ni-NTA chromatography) or RIPA buffer (anti-DVE-1 ChIP). The animals were lysed and the DNA fragmented to approximately 1 kilobase by sonication. Recovery of chromatin complexes was carried out by Ni-NTA affinity chromatography or by immunoprecipitation with the rabbit antiserum to DVE-1.

Quantitative real-time PCR was performed as described (Van Gilst et al., 2005). The promoter region of *hsp-60*, *hsp-6*, and *myo-2* was detected by PCR with primer pairs whose sequence is provided in Table S3: cehsp-60.5S & cehsp-60.10AS, C37H5.8.3S & C37H5.8.6AS, and myo-2.1S & myo-2.4AS. The coding region of *hsp-60*, *hsp-6*, and *myo-2* was detected by quantitative PCR using the MyIQ single-color real-time PCR detection system and IQ SYBR Green Supermix (Bio-Rad Laboratories) with the primer pairs cehsp-60.1S & cehsp-60.8AS, C37H5.8.3S & C37H5.6AS, and myo-2.1S & myo-2.2AS, respectively.

CLPP-1 Inhibition In Vitro and Worm Injection of CLPP-1 Inhibitors

hsp-16$_{pr}$::clpp-1^{WT}::TAG(zcIs21) V or N2 control animals were grown in liquid and incubated at 30°C for 6 hr to induce CLPP-1::TAG expression and allowed to recover at 20°C for 12 hr. Approximately 0.5 g of worms was purified by sucrose flotation and lysed, and CLPP-1::TAG was immunoprecipitated with anti-Myc (9E10) antibody. Suc-LLVY-AMC degradation was assayed in vitro in the absence or presence of MG132 (Sigma) or Z-LY-CMK (Bachem).

Z-LY-CMK, MG132, or the carrier DMSO solvent was injected into the pseudocoelomic space of immobilized young adult *ubl-5$_{pr}$::gfp* transgenic animals that had been raised at 16°C (or as a control, *aip-1$_{pr}$::gfp* transgenic animals). The injected animals were returned to 16°C or switched to 30°C. Six hours later, the animals were examined by fluorescence microscopy and the level of GFP fluorescence in the intestine was scored by a semiquantitative scale: 0, signal in nontransgenic animals; 1, faint fluorescence found in uninjected *ubl-5pr::gfp* animals at 16°C; 5, bright signal of uninjected animals at 30°C, with 2–4 reporting on grades in between.

Supplemental Data

Supplemental Data include six figures and three tables and can be found with this article online at http://www.developmentalcell.org/cgi/content/full/13/4/467/DC1/.

ACKNOWLEDGMENTS

We thank Gergana Dobreva and Rudolf Grosschedl (Max Planck Institute, Freiburg), Julia Flynn and Tania Baker (MIT), Shoei Mitani (National Bioresource Project for *C. elegans*, Tokyo, Japan), Richard Morimoto (Northwestern), and the *C. elegans* Genetics Center (Minneapolis, MN) for reagents. We also thank Barbara Conradt (Dartmouth), Marc Van Gilst (UCSF), Chris Lima (Memorial Sloan Kettering Institute), Chi Yun, Jeremy Nance, Jessica Treisman, and Scott Clark (Skirball Institute) for advice. Supported by NIH grants (DK47119 & ES08681), by the Ellison Medical Foundation, and by an NRSA to C.M.H. (F32-NS050901).

Received: March 12, 2007
Revised: June 25, 2007
Accepted: July 20, 2007
Published: October 9, 2007

REFERENCES

Barral, J.M., Broadley, S.A., Schaffar, G., and Hartl, F.U. (2004). Roles of molecular chaperones in protein misfolding diseases. Semin. Cell Dev. Biol. *15*, 17–29.

Benedetti, C., Haynes, C.M., Yang, Y., Harding, H.P., and Ron, D. (2006). Ubiquitin Like Protein 5 positively regulates chaperone gene expression in the mitochondrial unfolded protein response. Genetics *174*, 2229–2239.

Bukau, B., Weissman, J., and Horwich, A. (2006). Molecular chaperones and protein quality control. Cell *125*, 443–451.

Cai, S., Han, H.J., and Kohwi-Shigematsu, T. (2003). Tissue-specific nuclear architecture and gene expression regulated by SATB1. Nat. Genet. *34*, 42–51.

Dobreva, G., Dambacher, J., and Grosschedl, R. (2003). SUMO modification of a novel MAR-binding protein, SATB2, modulates immunoglobulin mu gene expression. Genes Dev. *17*, 3048–3061.

Flynn, J.M., Levchenko, I., Sauer, R.T., and Baker, T.A. (2004). Modulating substrate choice: the SspB adaptor delivers a regulator of the extracytoplasmic-stress response to the AAA+ protease ClpXP for degradation. Genes Dev. *18*, 2292–2301.

Fukushige, T., Brodigan, T.M., Schriefer, L.A., Waterston, R.H., and Krause, M. (2006). Defining the transcriptional redundancy of early bodywall muscle development in C. elegans: evidence for a unified theory of animal muscle development. Genes Dev. *20*, 3395–3406.

Gething, M.J., and Sambrook, J. (1992). Protein folding in the cell. Nature *355*, 33–45.

Gottesman, S. (2003). Proteolysis in bacterial regulatory circuits. Annu. Rev. Cell Dev. Biol. *19*, 565–587.

Guertin, D.A., Guntur, K.V., Bell, G.W., Thoreen, C.C., and Sabatini, D.M. (2006). Functional genomics identifies TOR-regulated genes that control growth and division. Curr. Biol. *16*, 958–970.

Hartl, F.U., and Neupert, W. (1990). Protein sorting to mitochondria: evolutionary conservations of folding and assembly. Science *247*, 930–938.

Hartl, F.U., and Hayer-Hartl, M. (2002). Molecular chaperones in the cytosol: from nascent chain to folded protein. Science *295*, 1852–1858.

Jagasia, R., Grote, P., Westermann, B., and Conradt, B. (2005). DRP-1-mediated mitochondrial fragmentation during EGL-1-induced cell death in C. elegans. Nature *433*, 754–760.

Kamath, R.S., Fraser, A.G., Dong, Y., Poulin, G., Durbin, R., Gotta, M., Kanapin, A., Le Bot, N., Moreno, S., Sohrmann, M., et al. (2003). Systematic functional analysis of the Caenorhabditis elegans genome using RNAi. Nature *421*, 231–237.

Kruger, E., Zuhlke, D., Witt, E., Ludwig, H., and Hecker, M. (2001). Clp-mediated proteolysis in Gram-positive bacteria is autoregulated by the stability of a repressor. EMBO J. *20*, 852–863.

Labrousse, A.M., Zappaterra, M.D., Rube, D.A., and van der Bliek, A.M. (1999). *C. elegans* dynamin-related protein DRP-1 controls severing of the mitochondrial outer membrane. Mol. Cell *4*, 815–826.

Lindquist, S. (1986). The heat-shock response. Annu. Rev. Biochem. *55*, 1151–1191.

Manning, B.D., and Cantley, L.C. (2003). Rheb fills a GAP between TSC and TOR. Trends Biochem. Sci. *28*, 573–576.

2006, lower row) were similarly injected and exposed to arsenite (4 mM) for 6 hr at 30°C to control for nonspecific suppressive effects of inhibitor injection on induced gene expression.

(D) Scheme of the hypothesized relationships of CLPP-1, DVE-1, and UBL-5 in the UPR^{mt}. CLPP-1 functions in an early mitochondrial step required for generation of the stress signal, whereas UBL-5 and DVE-1 function in a nuclear step. The latter is hypothesized to include the formation of a complex of UBL-5 and DVE-1 and association of DVE-1 with the promoters of genes encoding mitochondrial chaperones; the placement of UBL-5 in complex with the promoter-bound DVE-1 is entirely speculative.

Martinus, R.D., Garth, G.P., Webster, T.L., Cartwright, P., Naylor, D.J., Hoj, P.B., and Hoogenraad, N.J. (1996). Selective induction of mitochondrial chaperones in response to loss of the mitochondrial genome. Eur. J. Biochem. *240*, 98–103.

Nakagoshi, H., Hoshi, M., Nabeshima, Y., and Matsuzaki, F. (1998). A novel homeobox gene mediates the Dpp signal to establish functional specificity within target cells. Genes Dev. *12*, 2724–2734.

Neupert, W. (1997). Protein import into mitochondria. Annu. Rev. Biochem. *66*, 863–917.

Nijtmans, L.G., de Jong, L., Artal Sanz, M., Coates, P.J., Berden, J.A., Back, J.W., Muijsers, A.O., van der Spek, H., and Grivell, L.A. (2000). Prohibitins act as a membrane-bound chaperone for the stabilization of mitochondrial proteins. EMBO J. *19*, 2444–2451.

Nolden, M., Ehses, S., Koppen, M., Bernacchia, A., Rugarli, E.I., and Langer, T. (2005). The m-AAA protease defective in hereditary spastic paraplegia controls ribosome assembly in mitochondria. Cell *123*, 277–289.

Oh, S.W., Mukhopadhyay, A., Dixit, B.L., Raha, T., Green, M.R., and Tissenbaum, H.A. (2006). Identification of direct DAF-16 targets controlling longevity, metabolism and diapause by chromatin immunoprecipitation. Nat. Genet. *38*, 251–257.

Ron, D., and Walter, P. (2007). Signal integration in the endoplasmic reticulum unfolded protein response. Nat. Rev. Mol. Cell Biol. *8*, 519–529.

Sauer, R.T., Bolon, D.N., Burton, B.M., Burton, R.E., Flynn, J.M., Grant, R.A., Hersch, G.L., Joshi, S.A., Kenniston, J.A., Levchenko, I., et al. (2004). Sculpting the proteome with AAA(+) proteases and disassembly machines. Cell *119*, 9–18.

Stanhill, A., Haynes, C.M., Zhang, Y., Min, G., Steele, M.C., Kalinina, J., Martinez, E., Pickart, C.M., Kong, X.-P., and Ron, D. (2006). An arsenite-inducible regulatory particle-associated protein (AIRAP) adapts proteasomes to proteotoxicity. Mol. Cell *23*, 875–885.

Szyk, A., and Maurizi, M.R. (2006). Crystal structure at 1.9A of E. coli ClpP with a peptide covalently bound at the active site. J. Struct. Biol. *156*, 165–174.

Van Gilst, M.R., Hadjivassiliou, H., Jolly, A., and Yamamoto, K.R. (2005). Nuclear hormone receptor NHR-49 controls fat consumption and fatty acid composition in C. elegans. PLoS Biol. *3*, e53.

Voos, W., and Rottgers, K. (2002). Molecular chaperones as essential mediators of mitochondrial biogenesis. Biochim. Biophys. Acta *1592*, 51–62.

Wilkinson, C.R., Dittmar, G.A., Ohi, M.D., Uetz, P., Jones, N., and Finley, D. (2004). Ubiquitin-like protein Hub1 is required for pre-mRNA splicing and localization of an essential splicing factor in fission yeast. Curr. Biol. *14*, 2283–2288.

Yashiroda, H., and Tanaka, K. (2004). Hub1 is an essential ubiquitin-like protein without functioning as a typical modifier in fission yeast. Genes Cells *9*, 1189–1197.

Yoneda, T., Benedetti, C., Urano, F., Clark, S.G., Harding, H.P., and Ron, D. (2004). Compartment specific perturbation of protein folding activates genes encoding mitochondrial chaperones. J. Cell Sci. *117*, 4055–4066.

Young, L., Leonhard, K., Tatsuta, T., Trowsdale, J., and Langer, T. (2001). Role of the ABC transporter Mdl1 in peptide export from mitochondria. Science *291*, 2135–2138.

Zhao, Q., Wang, J., Levichkin, I.V., Stasinopoulos, S., Ryan, M.T., and Hoogenraad, N.J. (2002). A mitochondrial specific stress response in mammalian cells. EMBO J. *21*, 4411–4419.